Am J Cancer Res 2023;13(6):2488-2503
www.ajcr.us /ISSN:2156-6976/ajcr0150170

Original Article

The splicing factor proline and glutamine rich promotes the growth of osteosarcoma via the c-Myc signaling pathway

Lianghao Mao[1,2*], Pan Jiang[1,3*], Xuan Lei[1], Bing Zhang[1], Xinyu Zhong[1], Zhengyu Yin[1], Yongjie Wang[4], Dapeng Li[1], Yiming Zhang[1], Qiping Zheng[5,6]

[1]Affiliated Hospital of Jiangsu University, Zhenjiang 212001, Jiangsu, China; [2]Faculty of Medicine, Heidelberg University, Heidelberg 69120, Germany; [3]Guizhou Orthopedics Hospital, Guiyang 550002, Guizhou, China; [4]Department of Orthopedic Surgery, Shanghai Tenth People's Hospital Affiliated to Tongji University, Shanghai 200072, China; [5]Department of Laboratory Science, School of Medicine, Jiangsu University, Zhenjiang 212013, Jiangsu, China; [6]Shenzhen Walgenron Bio-Pharm Co., Ltd., Shenzhen 518118, Guangdong, China. [*]Equal contributors.

Received March 16, 2023; Accepted May 22, 2023; Epub June 15, 2023; Published June 30, 2023

Abstract: Splicing factor proline- and glutamine-rich (SFPQ) regulates transcripts in skeletal muscle metabolism and tumorigenesis. As osteosarcoma (OS) is the most common malignant bone tumor characterized by genome instability, such as MYC amplification, this study aimed to investigate the role and mechanism of SFPQ in OS. Expression of SFPQ in OS cell lines and human OS tissues was detected using quantitative real-time PCR, western blot, and fluorescence *in situ* hybridization (FISH) analyses. The oncogenic role of SFPQ in OS cells and murine xenograft models and the underlying mechanism of SFPQ on the c-Myc signaling pathway were assessed *in vitro* and *in vivo*. Results showed that SFPQ expression was upregulated and correlated with poor prognosis in OS patients. SFPQ overexpression promoted the malignant biological behavior of OS cells, while its knockdown markedly reduced the oncogenic function of OS. Additionally, depletion of SFPQ inhibited OS growth and bone destruction in nude mice. SFPQ overexpression induced malignant biological behaviors, which could be rescued by the depletion of c-Myc. These results suggest an oncogenic role of SFPQ in OS, possibly through the c-Myc signaling pathway.

Keywords: Splicing factor proline- and glutamine-rich (SFPQ), osteosarcoma, c-Myc signaling, progression

Introduction

Osteosarcoma (OS) is the most prevalent primary malignant bone cancer, with high morbidity and mortality rates. Its incidence has increased in recent decades, and it is especially prevalent among children 10-19 years old. OS is particularly common in Africa, Southeastern Asia, and South America [1]. The use of multimodality treatments, such as neoadjuvant chemotherapy, adjuvant chemotherapy, and limb salvage surgeries, has resulted in a rise in the 5-year survival rate of OS patients, approaching nearly 60% [2]. However, the histopathological responses to treatment can vary depending on factors such as age, gender, presence of metastasis, duration of symptoms, and tumor size after neoadjuvant chemotherapy [3, 4].

Genomic and epigenetic studies have made some progress in revealing the pathogenesis of OS. The pathogenetic features of OS are diverse and complex, including genomic disorders, oncogene, and tumor suppressor gene disorders, loss of DNA repair, and immune escape processes mediated by mesenchymal stem cells. Additionally, epigenetic events such as DNA methylation, histone modification, small nuclear remodeling, and non-coding RNA have been identified as potential risk factors leading to OS development [4-6]. The most common genome instabilities in OS are MYC amplification and TP53 mutation, which are closely associated with drug resistance and recurrence. However, the current treatment strategies are suboptimal, especially for patients with advanced OS and metastasis. Thus, there is an urgent need to investigate the underlying mech-

anisms from a fresh perspective and develop effective systematic therapies to improve patients' prognoses.

Splicing factor proline- and glutamine-rich (SFPQ) was discovered by JG Patton et al. in 1993 and was identified as a crucial protein required for the splicing of polypyrimidine binding protein (PTB) and its precursor mRNA [7]. As a DNA/RNA binding protein, SFPQ plays a necessary role in the alternative splicing process. As a heterodimer with Non-POU domain containing octamer binding (NONO), SFPQ is a basic splicing factor for precursor mRNA, regulating the early stage of spliceosome formation and catalysis step II [8]. Additionally, SFPQ is involved in DNA repair, mRNA splicing, fat formation, nerve regeneration, and even neurodegenerative diseases [9, 10]. Recent studies have found that SFPQ may be closely related to tumorigenesis and tumor progression. For example, SFPQ in complex with the splicing regulatory factor p54nrb/NONO can transform BIN1 into carcinogenic isoforms, enhancing hepatocellular carcinogenesis [11]. In renal cell carcinoma, human long non-coding RNA (lncRNA) SANT1 can cis-regulate the expression of SLC47A2 by changing the combination of SFPQ/E2F1/HDAC1 binding to the promoter region [12]. In colorectal cancer, MALAT1 binds to SFPQ and dissociates the SFPQ/PTBP2 dimer, releasing free PTBP2 and enhancing the translation of proto-oncogene RUNX2 [13]. In prostate cancer, SFPQ stabilizes and activates key lncRNA and androgen-regulated genes [14]. These findings suggest that SFPQ may be a potential target for developing novel treatments for tumors. However, the role and underlying mechanism of SFPQ in primary bone cancers, such as OS, remain to be investigated.

c-Myc is an oncogenic transcription factor and one of the most frequently dysregulated proto-oncogenes in human carcinogenesis [15]. Together with MYCL and MYCN, C-MYC belongs to the MYC family of genes, which encode c-Myc, L-Myc, and N-Myc, respectively. c-Myc is involved in the regulation of various cellular processes, such as tumor cell growth, DNA damage repair, epithelial-mesenchymal transition, autophagy, and cancer stem cell regeneration [16-20]. Moreover, c-Myc can stimulate tumor cell cycles and growth by upregulating the expression of cyclin-dependent kinases (CDKs) or interfering with the inhibitors of CDKs, such as p15, p21, and p27 [21].

c-Myc was first found to be amplified in OS cell lines by E Bogenmann et al. in 1987, and extensive expression of c-Myc was found both *in vitro* and *in vivo* [22]. Additionally, c-Myc plays a role in regulating energy metabolism and the differentiation and tumorigenic activity of bone marrow stromal cells in OS [16, 23, 24]. Furthermore, a recent multi-omics study, which included 121 primary OS patients, showed that MYC amplification was present in over half of OS patients, and overexpression of MYC may be the primary factor leading to poor survival [25]. Interestingly, W Shen et al. found that NEAT1 depletion attenuates nucleolar stress by relocating SFPQ, which facilitates c-Myc translation from nuclear paraspeckles to c-Myc mRNAs [26]. Moreover, Z Hu et al. revealed that NONO enhances tumorigenesis by switching the oncogenic isoform of MYC box-dependent interacting protein 1 in hepatic carcinoma through its interactions with SFPQ [27].

Considering that SFPQ, NONO, and NEAT1 are important components of paraspeckles [28] and may have a relationship with the c-Myc pathway in the carcinogenic process, we hypothesized that SFPQ plays a role in tumorigenesis by interacting with this pathway. To investigate this possibility, we conducted both *in vitro* and *in vivo* experiments to examine the role of SFPQ in OS and to elucidate the potential mechanism of the SFPQ-c-Myc pathway.

Materials and methods

Analysis of gene expression data and clinical information

We downloaded gene expression data and clinical information from two different sources for our analysis. For the GSE28424 microarray dataset [29], we used the R package GEOquery to download the data from the Gene Expression Omnibus (GEO) (https://www.ncbi.nlm.nih.gov/geo/) database [30] by using the R package GEOquery and the illuminaHumanv2.db R package to annotate the data. We created box plots using the R package "ggpubr" and the Wilcoxon test to compare two groups.

For the OS cohort in the Therapeutically Applicable Research To Generate Effective

Treatments (TARGET-OSA cohort), we downloaded the data from the Genomic Data Commons Data Portal (https://portal.gdc.cancer.gov/) using the R package TCGAbiolinks [31]. We used normalized transcripts per kilobase million (TPM) values for gene expression analyses and log2-transformed the values using an offset of 1 to prevent errors. Kaplan-Meier survival analyses were performed, and the results were visualized using the R packages "survival" and "survminer".

Patient selection and tissue microarray construction

We enrolled 70 patients with OS and obtained single normal bone and bone marrow tissues from the Affiliated Hospital of Jiangsu University. Written informed consent was obtained from each patient. The clinical research protocol was approved by the Ethics Committee of the Affiliated Hospital of Jiangsu University. Tissue microarray (TMA) construction was performed using all collected tissues. Clinical and histopathological data were available for all patients.

Fluorescence in situ hybridization (FISH)

We conducted FISH analysis on the TMAs using a commercially available SFPQ probe (Bioaitech, Xi'an, China) according to the manufacturer's protocol. The SFPQ probe, 5'-CY3-TGTGTGGCAAAGCGAACTCGAAGCTGTCT-CY3-3', was hybridized overnight to the specimens. Nuclei were counterstained with DAPI, and the specimens were analyzed using a Nikon inverted fluorescence microscope.

FISH analysis for SFPQ was evaluated based on the following scoring criteria: (1) intensity of fluorescence (0 for no staining, 1 for light staining, 2 for moderate staining, and 3 for strong staining) and (2) percentage of stained cells in the total number of tumor cells (0 for no staining, 1 for ≤ 25%, 2 for 26-49%, and 3 for ≥ 50%). The two scores were summed as the total score, and the average scores of each criterion in the TMAs were calculated. Qualitatively, scores > 2 were considered positive and scores ≤ 2 were considered negative.

Cell lines and cell culture

Three human OS cell lines (MG-63, MNNG/HOS, and U2OS) and the human osteoblastic cell line hFOB1.19 were purchased from the Cell Bank of the Chinese Academy of Sciences (Shanghai, China). All OS cell lines were cultured in Dulbecco's modified Eagle's medium (DMEM) (Gibco, NY, USA) containing 10% fetal bovine serum (FBS) (Gibco, NY, USA) and 1% penicillin/streptomycin at 37°C in a humidified incubator with 5% CO_2. The hFOB1.19 cells were cultured in DMEM/F-12 medium (Gibco, NY, USA) containing 10% FBS at 33.5°C with 5% CO_2.

Quantitative reverse-transcription polymerase chain reaction (qRT-PCR)

Total RNA was extracted from OS cells and hFOB1.19 cells using TRIzol reagent (Invitrogen, CA, USA) according to the manufacturer's instructions. The concentration and purity of RNA were measured using a NanoDrop 2000 spectrophotometer (Thermo Fisher Scientific, Waltham, MA, USA). RNA was reverse transcribed into cDNA with PrimeScript™ RT Master Mix (TaKaRa, Shiga, Japan). qRT-PCR was performed using SYBR Premix Ex Taq (TaKaRa, Shiga, Japan) according to the manufacturer's protocol in a StepOnePlus Real-Time PCR System (Applied Biosystems, Carlsbad, CA, USA). The expression levels of genes were normalized to the internal control gene GAPDH. The relative expression levels were calculated using the $2^{-\Delta\Delta Ct}$ method. The primer sequences are listed in **Table 1**.

Western blot

Total protein was extracted using RIPA buffer supplemented with protease inhibitors (Beyotime, Beijing, China). Equal amounts of protein samples were loaded onto 10% SDS-PAGE gels and transferred to polyvinylidene difluoride (PVDF) membranes. The membranes were blocked with 5% non-fat milk for 1 h at room temperature and then incubated with primary antibodies against human SFPQ (ab177149, Abcam, Cambridge, MA, USA), GAPDH (5174, Cell Signaling Technology, Danvers, MA, USA), c-Myc (ab32072, Abcam), and p27 (ab32034, Abcam) overnight at 4°C. Membranes were then incubated with HRP-conjugated corresponding secondary antibodies at room temperature for 1 h. Protein bands were detected with an enzyme-linked chemiluminescence (ECL) detection kit (Millipore, Burlington, MA,

Table 1. Primer sequences

Primer	Sequence (5' to 3')
GAPDH-F	GAAGGTGAAGGTCGGAGTC
GAPDH-R	GAAGATGGTGATGGGATTTC
SFPQ-F	AGCGATGTCGGTTGTTTGTTG
SFPQ-R	AGCGAACTCGAAGCTGTCTAC
C-MYC-F	GTCAAGAGGCGAACACACAAC
C-MYC-R	TTGGACGGACAGGATGTATGC

USA) and visualized using a Bio Imaging System (Bio-Rad, Hercules, CA, USA).

Plasmid, short hairpin RNA (shRNA), lentivirus, and cell transfection

To overexpress SFPQ, pcDNA 3.1 plasmids (Genepharma, Shanghai, China) targeting SFPQ (SFPQ cDNA) were used. The target sequences were SFPQ-F: CTTGGTACCGAGCTCGGATCCGCCACCATGTCTCGGGATCGGTTCCGGAGTCGTGGCGG; and SFPQ-R: TGCTGGATATCTGCAGAATTCCTAAAATCGGGGTTTTTTGTTTGGG. For knocking down the expression of SFPQ or C-MYC, siRNAs (si-SFPQ and si-C-MYC, respectively) were constructed by Genepharma with the following sequences: SFPQ forward 5'-GCAAAGGAUUCGGAUUUAUTT-3' and reverse 5'-AUAAAUCCGAAUCCUUUGCTT-3'. C-MYC forward 5'-GAACACACAACGUCUUGGATT-3' and reverse 5'-UCCAAGACGUUGUGUGUUCTT-3'. OS cells were transfected with SFPQ cDNA, empty vector (vector), siRNAs or siRNA-negative control (si-NC) using Lipofectamine 3000 Transfection Reagent (Invitrogen) according to the manufacturer's protocol.

Knockdown lentivirus LV16 was synthesized by Genepharma. The infection efficiency was evaluated by qRT-PCR and western blot analyses. MNNG-HOS cells were transfected with LV16 lentivirus vector encoding a shRNA sequence of SFPQ: 5'-GGCACGTTTGAGTACGAATAT-3'. Puromycin was used to select and culture infected cells for stable expression of OS cell lines.

Cell migration and invasion

Migration and invasion assays were performed using Transwell chambers with 8-um pores (Corning, Corning, NY, USA). For the migration assay, 4×10^4 OS cells were suspended in 200 μl of serum-free medium and transferred into the upper Transwell chamber. For the invasion assay, Matrigel (BD Bioscience, San Jose, CA, USA) was coated onto the upper chamber beforehand, and then 8×10^4 OS cells were suspended in 200 μl of serum-free medium and seeded into the upper chamber. The cells were cultured in an atmosphere with 5% CO_2 at 37°C for 24 h after adding 600 μl of medium containing 10% serum to the lower chamber. After incubation, the OS cells were fixed with 4% paraformaldehyde for 30 min and stained with 0.1% crystal violet for 45 min. The stain was then extracted for imaging and counting using an inverted Olympus microscope.

Cell proliferation and EdU assays

For cell proliferation assays, 4×10^3 cells treated under different conditions were seeded into each well of 96-well plates and cultured for 24 h. Then, 10 μl of water-soluble tetrazolium salt from a Cell Counting Kit-8 (CCK-8, Dojindo, Japan) were added into each well and the cells were further incubated at 37°C with 5% CO_2 for 1 h. The absorbance was measured at 450 nm using a spectrophotometer. The proliferation rate of OS cells was measured at 0, 24, 48, 72, and 96 h.

To perform EdU assays, cells were incubated with 50 μM EdU reagent in 96-well plates according to the manufacturer's protocol (Riobio). Nuclei were stained with Hoechst stain and the results were recorded using fluorescence microscopy.

Cell cycle analysis

Cell cycle analysis was conducted using a BD Cycletest Plus DNA reagent kit (BD Bioscience) and flow cytometry analysis. Cells were collected, washed with PBS, and fixed in ice-cold 70% ethanol overnight at 4°C. After being washed twice with cold PBS, the fixed cells were incubated with 500 μl propidium iodide staining solution at room temperature. At least 1,000 OS cells from each sample were counted using flow cytometry to measure the cell cycle. The percentage of cells in each phase was evaluated using ModFit LT software.

Murine models and tumor imaging

All animal experiments were conducted in accordance with the guidelines of the National

Institutes of Health Guide for the Care and Use of Laboratory Animals and were approved by the Ethics Committee of Jiangsu University. MNNG-HOS cells transfected with si-SFPQ or si-negative control (si-NC) were used in this study. A total of 24 male nude mice aged 4 weeks were purchased from GemPharmatech (Nanjing, China) and were randomly divided into four groups (n = 6 per group).

In subcutaneous xenograft experiments, 2×10^6 transfected OS cells were injected into the right back of 4-week-old nude mice. In orthotopic xenograft experiments, 2×10^6 transfected OS cells were injected into the marrow cavity of the right tibia. Metastatic conditions were measured using an *in vivo* imaging system (Caliper Life Sciences, Inc., Waltham, MA, USA). The weight and tumor size of each nude mouse were measured every 3 days for one month post-injection. Tumor volume was calculated using the following formula: $V = 1/2 \times L \times W^2$ (where L is tumor length and W is tumor width).

Upon sacrifice of the mice, the tumors were removed for hematoxylin-eosin (H&E) staining, micro-computed tomography (CT), and immunohistochemistry (IHC) staining analyses.

Histopathology and IHC

Paraffin-embedded OS tissue samples were cut into 5-μm sections. The primary tumors and lung sections were first stained with H&E and then immunostained using specific antibodies, including anti-SFPQ (15585-1-AP, 1:100, Proteintech) and anti-c-Myc (ab32072, 1:100, Abcam) as previously described [32].

Statistical analysis

The results of the *in vitro* assays are presented as means ± standard deviation (SD) from at least three independent experiments. Student's t tests were conducted using GraphPad Prism 5.0 (GraphPad Software Inc., USA) to determine significant differences between two groups. One-way ANOVA was used to analyze data from more than two groups. Statistical significance was defined as $P < 0.05$. GraphPad Prism software Version 8.0 was used to assess statistical differences.

Results

SFPQ expression is associated with poor clinicopathological features in OS patients

To investigate SFPQ expression in OS, we initially conducted a bioinformatics analysis to analyze its expression in OS patients. The results indicated that SFPQ overexpression was significantly associated with poor OS patient survival ($P < 0.05$, **Figure 1A**, **1B**). Compared to bone marrow from a healthy donor, SFPQ mRNA expression was higher in bone marrow from OS patients based on sequencing data from the GSE28424 microarray data (**Figure 1C**). We further confirmed SFPQ expression in OS patients by conducting FISH analysis on OS tissue microarrays. SFPQ was also overexpressed in OS tissues (**Figure 1D**) and was significantly associated with patients' age (**Table 2**).

SFPQ is overexpressed in human OS cell lines

To explore SFPQ expression in OS cell lines, we extracted mRNA and protein from human osteoblastic cells (hFOB1.19) and three OS cell lines (MG-63, MNNG/HOS, and U2OS). qRT-PCR and western blot analysis revealed that SFPQ was significantly overexpressed in the OS cell lines compared to hFOB1.19 cells (**Figure 1E**, **1F**).

SFPQ knockdown suppresses the growth of OS cells in vitro

To investigate the role of SFPQ in OS cells, we knocked down its expression in MNNG-HOS and U2OS cell lines by transfecting them with si-SFPQ, which was confirmed by qRT-PCR and western blot (**Figure 2A**, **2B**). The effect of SFPQ knockdown on cell proliferation was assessed using CCK-8 assays, which showed that the proliferation of OS cells was significantly inhibited in a time-dependent manner (**Figure 2C**). The inhibitory effect on proliferation was further confirmed by EdU assays, which showed a reduction in the number of proliferating cells transfected with si-SFPQ compared to those transfected with si-NC (**Figure 2D**).

To study the effect of SFPQ knockdown on migration and invasion, Transwell assays were performed. The number of migrated and invaded OS cells was significantly reduced in the si-

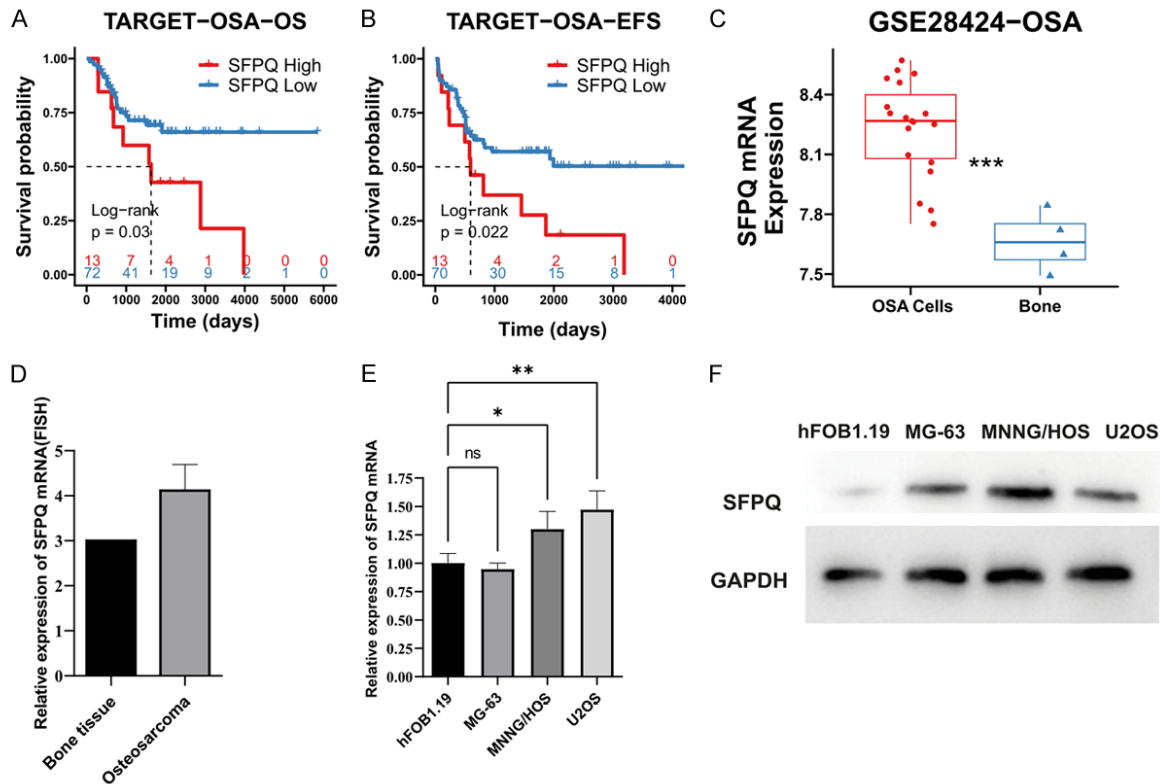

Figure 1. SFPQ is overexpressed in osteosarcoma (OS) and correlates with poor OS patient survival. A, B. High SFPQ expression is associated with poor overall survival (TARGET-OSA-OS) and event-free survival (TARGET-OSA-EFS) in OS patients based on data from TARGET databases. C. SFPQ is highly expressed in OS tumor cells compared to bone tissue based on the GSE28424 microarray dataset. D. SFPQ is highly expressed in OS tumors compared to normal bone tissue based on fluorescence *in situ* hybridization (FISH) analyses. E, F. qRT-PCR and western blot analyses demonstrated the overexpression of SFPQ in OS cell lines (MG-63, MNNG/HOS, and U2OS) compared to the human osteoblastic cell line hFOB1.19. Data are presented as means ± SD of three independent experiments. ***$P < 0.001$, **$P < 0.01$, and *$P < 0.05$.

SFPQ group compared to the si-NC group (**Figure 2E**, **2F**). Flow cytometry analysis of cell cycle distribution revealed a significant G2 cell cycle arrest in OS cells transfected with si-SFPQ compared to those transfected with si-NC (**Figure 2G**). These findings indicate that the knockdown of SFPQ suppresses the growth of OS cells *in vitro* and suggest potential roles for SFPQ in regulating OS cell proliferation, migration, and invasion.

SFPQ overexpression promotes OS cell growth in vitro

The overexpression efficacy of pcDNA 3.1 encoding SFPQ cDNA was confirmed by qRT-PCR and western blot analyses in OS cells, which revealed that SFPQ expression was upregulated in these cells (**Figure 3A**, **3B**). To investigate the effect of SFPQ overexpression on the biological behaviors of OS cells, we performed CCK-8 and EdU assays to evaluate cell proliferation and Transwell migration and invasion assays to evaluate cell migration and invasion, respectively. Our findings demonstrated that SFPQ overexpression significantly increased proliferation activity (**Figure 3C**, **3D**) and promoted migration and invasion (**Figure 3E**, **3F**) in OS cells. Overall, these findings suggest that SFPQ plays a role in promoting the malignant biological behaviors of OS cells *in vitro*.

SFPQ activates c-Myc expression in OS

As a previous study reported that SFPQ can act as an IRES trans-acting factor and bind to the IRES of c-Myc to regulate its translation [33], we hypothesized that SFPQ may also regulate c-Myc expression and function in OS. To test

Table 2. Association of SFPQ expression with clinical characteristics of osteosarcoma patients

Characteristics	SFPQ mRNA levels		
	High	Low	*P*-value
Age, years			
< 18	19	4	0.0122*
≥ 18	46	1	
Gender			
Male	43	2	0.6256
Female	21	3	
Tumor size (cm)			
T1	30	3	0.752
T2+T3	35	2	
Lymph node metastasis			
N0	60	4	0.2158
N1	5	1	
Stage			
I-II	60	4	0.2158
III-IV	5	1	
Location			
Lower limb	52	5	0.0618
Upper limb	18	0	

*Statistically significant.

this, we performed qRT-PCR and western blot analyses to assess whether SFPQ could influence the expression of c-Myc *in vitro*. The results showed that SFPQ overexpression led to increased c-Myc mRNA and protein expression (**Figure 4A**, **4B**). Conversely, SFPQ knockdown led to decreased c-Myc mRNA expression, while c-Myc protein expression did not change significantly (**Figure 4B**). Additionally, SFPQ inhibition upregulated the protein expression of the tumor suppressor p27, while SFPQ upregulation decreased its expression (**Figure 4B**). These findings support our hypothesis that SFPQ plays an oncogenic role in regulating c-Myc expression in OS tumorigenesis.

c-Myc inhibition rescues the effect of SFPQ overexpression in OS cells

To investigate whether SFPQ plays an oncogenic role in OS via the c-Myc pathway, we first transfected MNNG/HOS and U2OS cells with si-C-MYC to knockdown c-Myc expression. We then transfected the SFPQ-pcDNA 3.1 plasmid into the c-Myc knockdown cells to investigate the function of c-Myc on SFPQ. After overexpressing SFPQ using SFPQ cDNA, we knocked down c-Myc and confirmed by western blot analysis that the knockdown of c-Myc decreased the expression of SFPQ (**Figure 4C**). Furthermore, inhibition of c-Myc significantly attenuated the effects of SFPQ overexpression on the migration (**Figure 4D**) and invasion (**Figure 4E**) of OS cells. These results suggest that SFPQ promotes the oncogenic functions of OS cells via the c-Myc pathway.

SFPQ inhibition suppresses OS growth in vivo via the c-Myc pathway

To confirm the effect of SFPQ *in vivo*, we established xenograft OS models in nude mice. MNNG/HOS cells were transfected with lentivirus encoding sh-SFPQ or sh-NC, and stably transfected OS cells were screened using puromycin. SFPQ inhibition significantly suppressed tumor size and weight in subcutaneous xenograft models compared to the negative control group (**Figure 5A**). To comprehensively verify the function of SFPQ *in vivo*, we also established orthotopic xenograft models in nude mice. SFPQ inhibition led to a significant reduction in tumor growth in the SFPQ knockdown group (**Figure 5B**), similar to the subcutaneous model. H&E staining showed fewer tumor cells and immune cell infiltration in the sh-SFPQ group compared with the sh-NC group (**Figure 5C**). IHC analysis showed relatively less expression of SFPQ and c-Myc in tumor cells in the SFPQ knockdown group (**Figure 5D**, **5E**). Furthermore, micro-CT showed less tumor bone erosion in the SFPQ knockdown group compared to the control group (**Figure 5F**). These results strongly support the oncogenic role of SFPQ in cancer and suggest that its mechanism of action might involve targeting the c-Myc pathway to promote OS progression.

Discussion

SFPQ is a crucial splicing factor that plays a significant role in the regulation of signal-induced alternative splicing. As a DNA and RNA binding protein, SFPQ is also involved in several nuclear processes [34], making it an essential molecule for proper cellular function. With ubiquitous expression in bone marrow, skin, and other tissues such as lymph nodes, endometrium, and appendix [35], the involvement of SFPQ in various cellular processes has become increasingly apparent. Recent evidence indi-

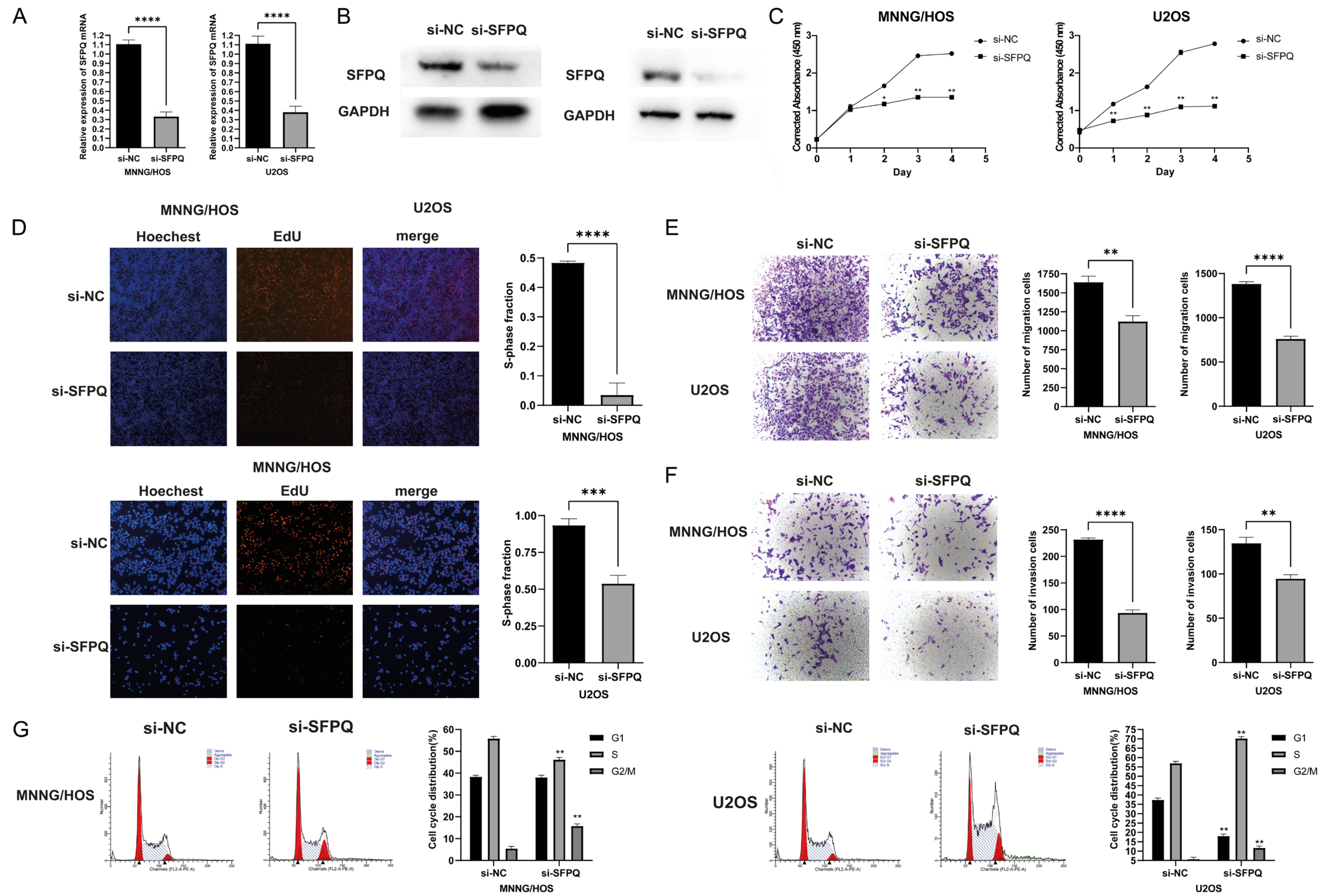

Figure 2. Knockdown of SFPQ inhibits osteosarcoma (OS) cell growth. A, B. qRT-PCR and western blot analyses demonstrated reduced SFPQ expression upon transfection with si-SFPQ compared to cells transfected with the negative control siRNA (si-NC). C, D. Knockdown of SFPQ inhibited OS cell proliferation as observed in CCK-8 and EdU assays. E, F. SFPQ knockdown suppressed OS cell migration and invasion in Transwell migration and invasion assays. G. Knockdown of SFPQ expression in OS cells resulted in cell cycle arrest in the G2 phase compared with si-NC cells. Data are presented as means ± SD of three independent experiments. ****P < 0.0001, **P < 0.01, *P < 0.05.

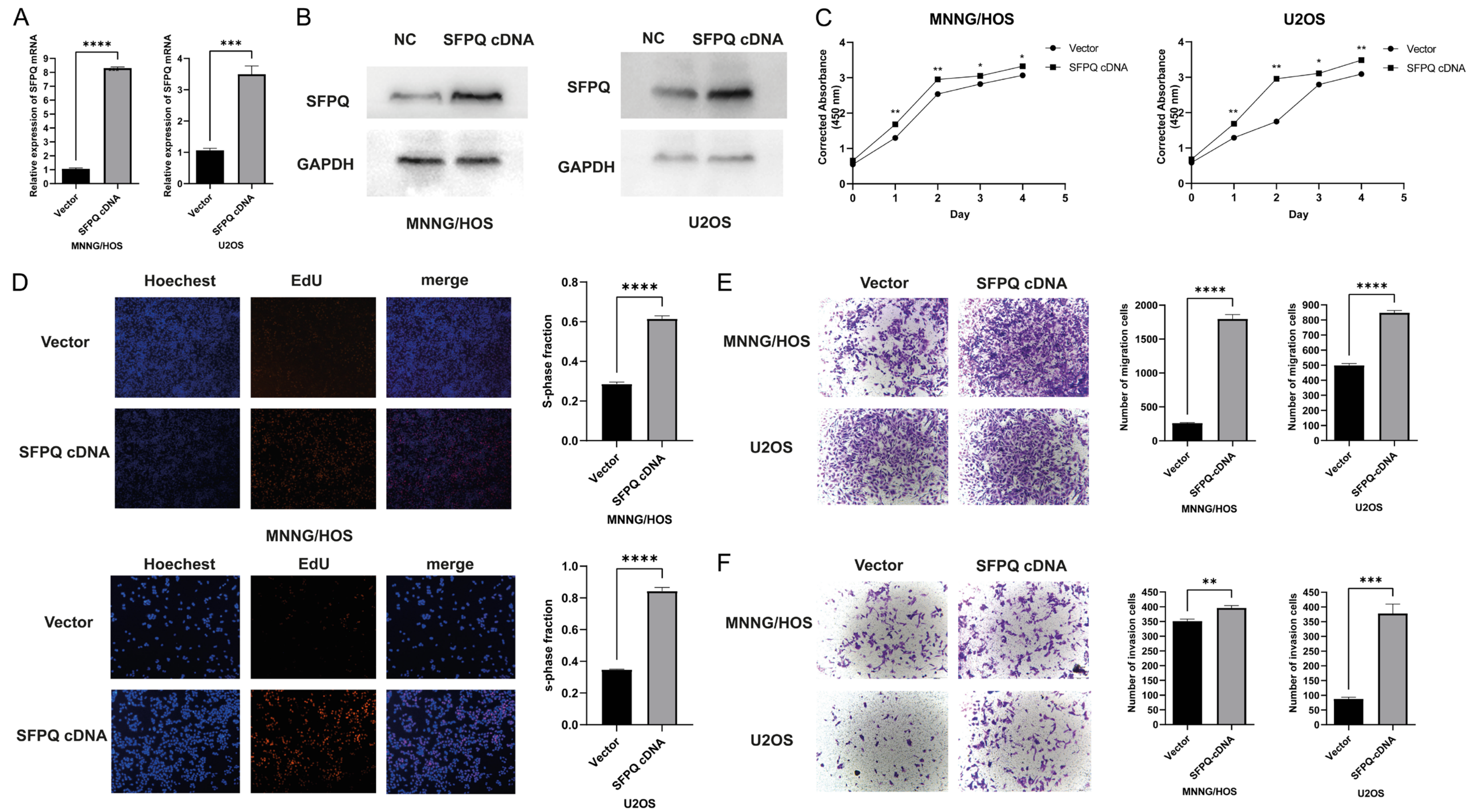

Figure 3. SFPQ overexpression promotes osteosarcoma (OS) cell growth. A, B. qRT-PCR and western blot analyses demonstrated that SFPQ was overexpressed following transfection with SFPQ cDNA compared to negative control (NC; vector) cells. C, D. SFPQ overexpression enhanced OS cell proliferation as observed in CCK-8 and EdU assays. E, F. SFPQ overexpression facilitated OS cell migration and invasion in Transwell migration and invasion assays. Data are presented as means ± SD of three independent experiments. ****$P < 0.0001$, ***$P < 0.001$, **$P < 0.01$, *$P < 0.05$.

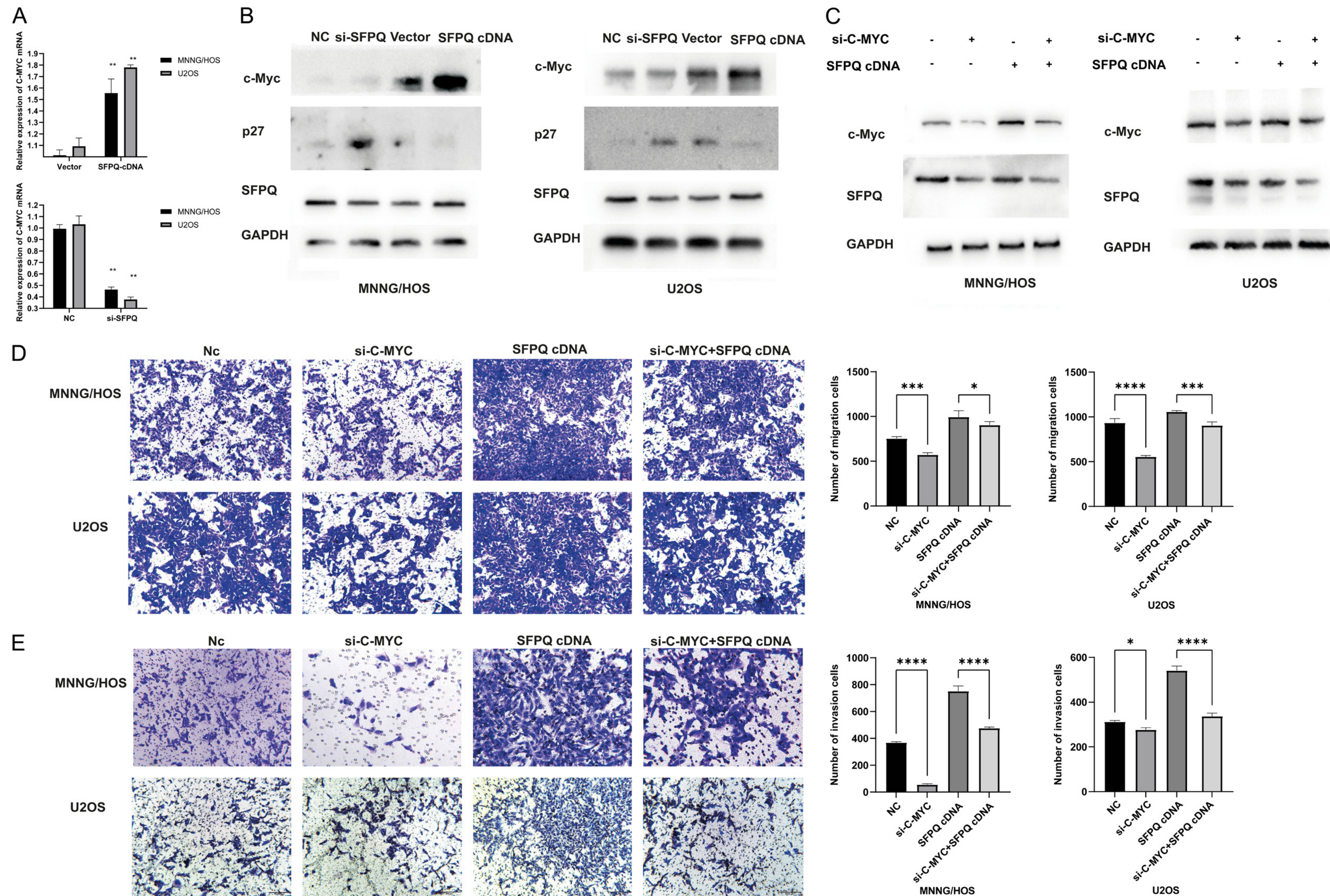

Figure 4. c-Myc knockdown rescued the oncogenic functions induced by SFPQ overexpression in osteosarcoma (OS) cells. A, B. qRT-PCR and western blot analyses demonstrated a correlation between SFPQ with c-Myc expression. NC, negative control. C. c-Myc knockdown enhanced SFPQ expression following transfection with SFPQ cDNA. D, E. c-Myc knockdown rescued OS cell migration and invasion induced by SFPQ overexpression in Transwell migration and invasion assays. Data are presented as mean ± SD of three independent experiments. ****P < 0.0001, ***P < 0.001, *P < 0.05.

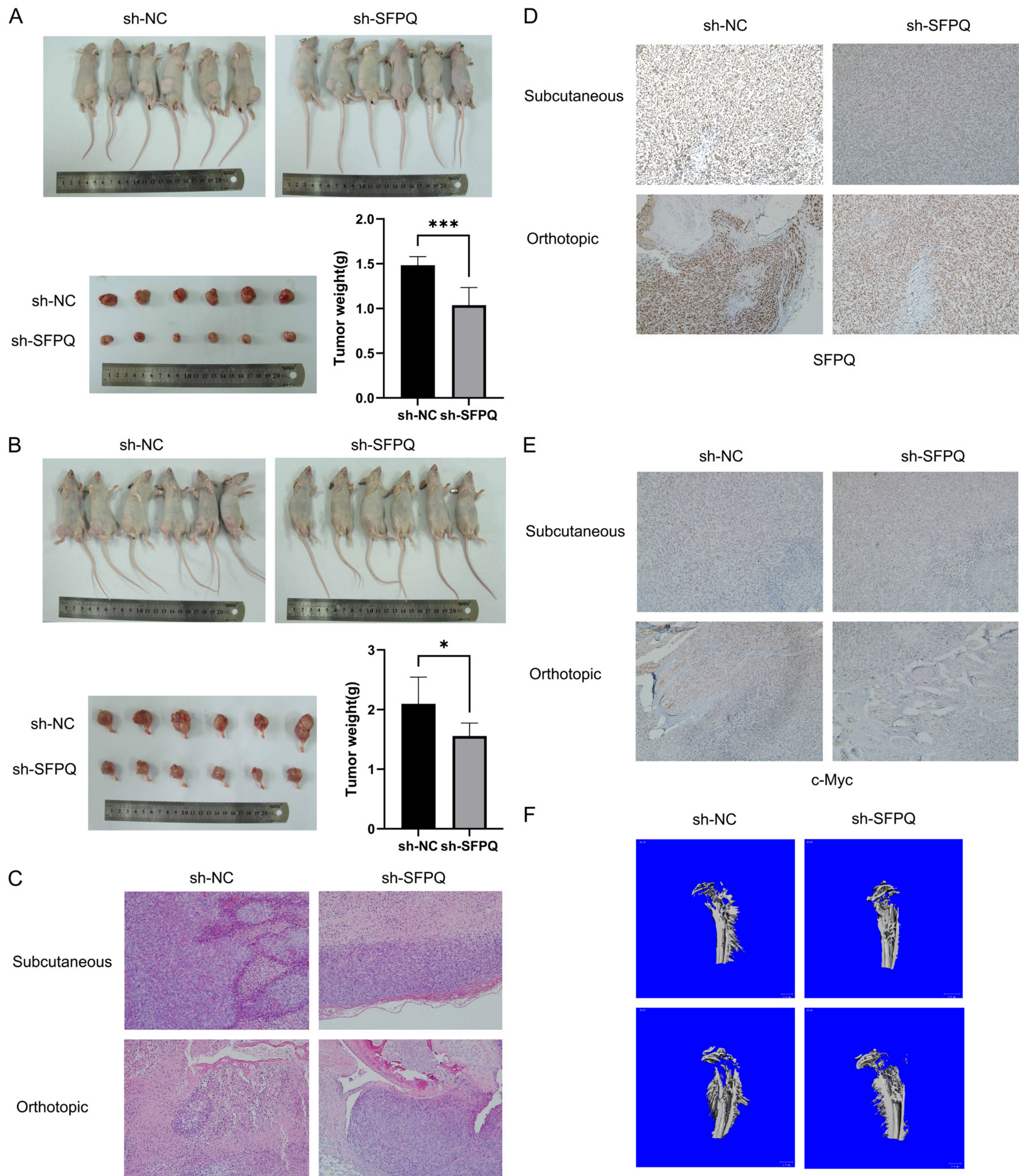

Figure 5. SFPQ knockdown inhibited osteosarcoma (OS) tumor progression *in vivo* through targeting of c-Myc. After stable expression of sh-SFPQ or sh-NC, OS cells were injected into nude mice. Tumor size and weight were significantly suppressed in the sh-SFPQ group compared to the NC group in both subcutaneous (A) and orthotopic xenograft models (B). (C) H&E staining demonstrated reduced numbers of tumor cells and infiltrated immune cells in the sh-SFPQ group compared to the sh-NC group. (D, E) Immunostaining of subcutaneous and orthotopic tumors with SFPQ and c-Myc antibodies confirmed differential protein expression. (F) Micro-computed tomography analysis indicated reduced bone erosion in the sh-SFPQ group compared to the sh-NC group. ***$P < 0.001$, and *$P < 0.05$.

cates that SFPQ may play a role in tumorigenesis [36-40]. Moreover, SFPQ also facilitates the translation of c-Myc by relocating from nuclear paraspeckles to c-Myc mRNAs [26]. c-Myc is a transcription factor that is constitutively and aberrantly expressed in almost 70% of human cancers, promoting the survival of cancer cells [15]. Therefore, we hypothesize that SFPQ may

also play a role in the pathogenesis of OS via the c-Myc pathway.

In our study, we used bioinformatics to analyze the expression of SFPQ in OS patients and found that it was overexpressed and associated with OS patient survival. We confirmed SFPQ overexpression in OS patients through FISH analysis, which demonstrated that SFPQ was overexpressed in OS patient tissues compared to normal osteoblasts. Additionally, we evaluated SFPQ mRNA and protein expression in OS cell lines and observed that SFPQ was also overexpressed in these cells. Notably, knocking down SFPQ significantly inhibited the proliferation, migration, and invasion of OS cells and arrested the cell cycle. Conversely, overexpressing SFPQ promoted the biological activities of OS cells.

Our *in vivo* experiments also supported our findings, as knockdown of SFPQ inhibited tumor growth in orthotopic OS xenograft models. Overall, these results suggest that SFPQ may play a crucial role in regulating OS. A previous study found that the depletion of SFPQ can inhibit proliferation and induce S-phase arrest and apoptosis in colorectal and melanoma cells [36]. Furthermore, SFPQ may protect cancer cells from platinum-induced death by promoting chemoresistance through alternative splicing mechanisms [38]. These studies highlight that SFPQ may promote OS tumorigenesis and cancer progression through multiple mechanisms.

OS is characterized by the dysregulation of oncogenic genes, which can contribute to its pathogenesis. Abnormal alternative splicing events are a crucial factor in the development of OS [41, 42]. As the primary splicing factor, SFPQ may promote OS by regulating the splicing events of specific genes that have the potential to drive tumorigenesis. For instance, there is an association between disease progression and aberrant alternative splicing events of the leptin receptor in OS [43]. TP53 is the most commonly mutated gene in human cancers, and the germline rearrangement in intron 1 of TP53 is frequently observed in OS [44]. Lnc-KASRT can modify SRSF1-related KLF6 alternative splicing, leading to its oncogenic activity in OS [45]. SRSF3, a proto-oncogene and splicing factor, regulates splicing events that control the expression of multiple oncogenic or tumor-suppressive genes, thereby maintaining cell homeostasis in OS [46]. Alterations of spliceosome proteins can affect specific splicing events, tumor cell motility, and metastatic progression, leading to the instability of the OS proteome [47]. Moreover, aberrant alternative splicing is also involved in the response to DNA damage in OS [48]. SFPQ, along with NONO, SRSF1, and SRSF3, belongs to a group of vital splicing factors that interact with each other and may collectively play important roles in tumorigenesis [49-51]. Given the close connection between aberrant splicing events and OS progression, SFPQ might synergistically work with other splicing factors such as serine/arginine (SR)-rich proteins to promote OS development by regulating the expression of vital genes.

c-Myc, an oncogenic transcription factor and one of the most common proto-oncogenes in human carcinogenesis [15, 52], plays a significant role in tumor cell growth, DNA damage repair, epithelial-mesenchymal transition, autophagy, and tumor stem cell regeneration [17-20]. It belongs to the Myc family of proteins, which includes c-Myc, L-Myc, and N-Myc that are encoded by the genes MCYC, MYCL, and MYCN, respectively. The overexpression of c-Myc can stimulate tumor cell cycle progression and tumor growth by upregulating CDKs or interfering with CDK inhibitors such as p15, p21, and p27 [21]. In OS, c-Myc overexpression has been associated with bone marrow stromal cell transformation, chemoresistance, and tumor progression [24, 53, 54].

Recent studies have shed light on the potential interaction between SFPQ and c-Myc in various cancer types. The relationship between SFPQ and c-Myc was initially explored in colorectal cancer, where SFPQ expression correlated with the expression of c-Myc, cyclin D1, and cyclin D4 [55]. Furthermore, the depletion of NEAT1 lncRNA can enhance c-Myc translation by promoting the release of SFPQ, which binds to the internal ribosome entry site of c-Myc [56]. These findings highlight the intricate interplay between SFPQ and c-Myc in modulating gene expression and cellular processes. However, the specific interaction and mechanism between SFPQ and c-Myc remain unknown.

Our study investigated the influence of SFPQ on c-Myc mRNA and protein expression in OS cell

lines. We observed that SFPQ enhanced both the mRNA and protein expression of c-Myc, while depletion of SFPQ resulted in decreased c-Myc mRNA expression. In xenograft mouse models, the depletion of SFPQ led to reduced c-Myc expression, as determined by IHC analysis. Additionally, inhibition of c-Myc rescued the enhanced oncogenic behaviors induced by SFPQ overexpression. These findings establish a correlation between SFPQ and c-Myc in OS, providing new insights into the understanding of cancer pathogenesis.

It is important to acknowledge certain limitations in our study. We did not investigate the binding relationship between SFPQ and c-Myc from the perspective of alternative splicing, which requires further investigation in future studies. Understanding the precise mechanism underlying the interaction between SFPQ and c-Myc, particularly in the context of alternative splicing, will contribute to a more comprehensive understanding of their roles in OS and potentially uncover new therapeutic targets.

Conclusion

This study provides evidence confirming the crucial role of SFPQ as an oncogenic factor in OS. The findings demonstrate its association with poor OS patient survival and its ability to promote OS growth both in vitro, using OS cell lines, and in vivo, through the utilization of mouse xenograft models. Notably, the mechanism underlying its oncogenic function involves the targeting of the c-Myc pathway. These novel insights into the pathogenesis of OS shed light on potential therapeutic targets for future treatment strategies. Further investigation and exploration of SFPQ and its interactions within the context of OS may yield valuable advancements in the field of OS research.

Acknowledgements

This work was supported by the National Natural Science Foundation of China (No. 81601931; 81672229), the Natural Science Foundation of Jiangsu Province (BK20150475), the Youth Medical Key Talent Project of Jiangsu (QNRC2016844), "Six One Projects" for high-level health professionals in Jiangsu Province Top Talent Project (LGY2019089), Jiangsu Provincial key research and development program (BE2020679), Medical Education Collaborative Innovation Fund Of Jiangsu University (JDY-2022001), Jiangsu Province Postgraduate Practice Innovation Program (No. SJCX20_1434), Zhenjiang City social development project (SH2023018), and the Shenzhen Science and Technology Program (No.KQTD20170810154-011370).

Disclosure of conflict of interest

None.

Address correspondence to: Drs. Dapeng Li and Yiming Zhang, Affiliated Hospital of Jiangsu University, Zhenjiang 212001, Jiangsu, China. E-mail: lidapeng706@hotmail.com (DPL); zhangyiming0607@163.com (YMZ); Dr. Qiping Zheng, Department of Laboratory Science, School of Medicine, Jiangsu University, Zhenjiang 212013, Jiangsu, China. E-mail: qp_zheng@hotmail.com

References

[1] Rojas GA, Hubbard AK, Diessner BJ, Ribeiro KB and Spector LG. International trends in incidence of osteosarcoma (1988-2012). Int J Cancer 2021; 149: 1044-1053.
[2] Siegel RL, Miller KD and Jemal A. Cancer statistics, 2018. CA Cancer J Clin 2018; 68: 7-30.
[3] Prabowo Y, Setiawan I, Kamal AF, Kodrat E and Labib Zufar ML. Correlation between prognostic factors and the histopathological response to neoadjuvant chemotherapy in osteosarcoma: a retrospective study. Int J Surg Oncol 2021; 2021: 8843325.
[4] Otoukesh B, Boddouhi B, Moghtadaei M, Kaghazian P and Kaghazian M. Novel molecular insights and new therapeutic strategies in osteosarcoma. Cancer Cell Int 2018; 18: 158.
[5] Zheng Y, Wang G, Chen R, Hua Y and Cai Z. Mesenchymal stem cells in the osteosarcoma microenvironment: their biological properties, influence on tumor growth, and therapeutic implications. Stem Cell Res Ther 2018; 9: 22.
[6] Tian W, Li Y, Zhang J, Li J and Gao J. Combined analysis of DNA methylation and gene expression profiles of osteosarcoma identified several prognosis signatures. Gene 2018; 650: 7-14.
[7] Patton JG, Porro EB, Galceran J, Tempst P and Nadal-Ginard B. Cloning and characterization of PSF, a novel pre-mRNA splicing factor. Genes Dev 1993; 7: 393-406.
[8] Yarosh CA, Iacona JR, Lutz CS and Lynch KW. PSF: nuclear busy-body or nuclear facilitator? Wiley Interdiscip Rev RNA 2015; 6: 351-367.
[9] Shav-Tal Y and Zipori D. PSF and p54(nrb)/NonO--multi-functional nuclear proteins. FEBS Lett 2002; 531: 109-114.

[10] Mugabo Y, Sadeghi M, Fang NN, Mayor T and Lim GE. Elucidation of the 14-3-3zeta interactome reveals critical roles of RNA-splicing factors during adipogenesis. J Biol Chem 2018; 293: 6736-6750.
[11] Hu Z, Dong L, Li S, Li Z, Qiao Y, Li Y, Ding J, Chen Z, Wu Y, Wang Z, Huang S, Gao Q, Zhao Y and He X. Splicing regulator p54nrb/non-POU domain-containing octamer-binding protein enhances carcinogenesis through oncogenic isoform switch of MYC box-dependent interacting protein 1 in hepatocellular carcinoma. Hepatology 2020; 72: 548-568.
[12] Gao Z, Chen M, Tian X, Chen L, Chen L, Zheng X, Wang H, Chen J, Zhao A, Yao Q, Zhu Q, Jin S, Hu H, Zeng S and Yu L. A novel human lncRNA SANT1 cis-regulates the expression of SLC47A2 by altering SFPQ/E2F1/HDAC1 binding to the promoter region in renal cell carcinoma. RNA Biol 2019; 16: 940-949.
[13] Ji Q, Cai G, Liu X, Zhang Y, Wang Y, Zhou L, Sui H and Li Q. MALAT1 regulates the transcriptional and translational levels of proto-oncogene RUNX2 in colorectal cancer metastasis. Cell Death Dis 2019; 10: 378.
[14] Takayama KI, Suzuki T, Fujimura T, Yamada Y, Takahashi S, Homma Y, Suzuki Y and Inoue S. Dysregulation of spliceosome gene expression in advanced prostate cancer by RNA-binding protein PSF. Proc Natl Acad Sci U S A 2017; 114: 10461-10466.
[15] Madden SK, de Araujo AD, Gerhardt M, Fairlie DP and Mason JM. Taking the Myc out of cancer: toward therapeutic strategies to directly inhibit c-Myc. Mol Cancer 2021; 20: 3.
[16] Shen S, Yao T, Xu Y, Zhang D, Fan S and Ma J. CircECE1 activates energy metabolism in osteosarcoma by stabilizing c-Myc. Mol Cancer 2020; 19: 151.
[17] Saenz DT, Fiskus W, Mill CP, Perera D, Manshouri T, Lara BH, Karkhanis V, Sharma S, Horrigan SK, Bose P, Kadia TM, Masarova L, DiNardo CD, Borthakur G, Khoury JD, Takahashi K, Bhaskara S, Lin CY, Green MR, Coarfa C, Crews CM, Verstovsek S and Bhalla KN. Mechanistic basis and efficacy of targeting the β-catenin-TCF7L2-JMJD6-c-Myc axis to overcome resistance to BET inhibitors. Blood 2020; 135: 1255-1269.
[18] Dong H, Adams NM, Xu Y, Cao J, Allan DSJ, Carlyle JR, Chen X, Sun JC and Glimcher LH. The IRE1 endoplasmic reticulum stress sensor activates natural killer cell immunity in part by regulating c-Myc. Nat Immunol 2019; 20: 865-878.
[19] Gu Y, Zhang J, Ma X, Kim BW, Wang H, Li J, Pan Y, Xu Y, Ding L, Yang L, Guo C, Wu X, Wu J, Wu K, Gan X, Li G, Li L, Forman SJ, Chan WC, Xu R and Huang W. Stabilization of the c-Myc protein by CAMKIIγ promotes T cell lymphoma. Cancer Cell 2017; 32: 115-128, e117.
[20] Abraham SA, Hopcroft LE, Carrick E, Drotar ME, Dunn K, Williamson AJ, Korfi K, Baquero P, Park LE, Scott MT, Pellicano F, Pierce A, Copland M, Nourse C, Grimmond SM, Vetrie D, Whetton AD and Holyoake TL. Dual targeting of p53 and c-MYC selectively eliminates leukaemic stem cells. Nature 2016; 534: 341-346.
[21] García-Gutiérrez L, Bretones G, Molina E, Arechaga I, Symonds C, Acosta JC, Blanco R, Fernández A, Alonso L, Sicinski P, Barbacid M, Santamaría D and León J. Myc stimulates cell cycle progression through the activation of Cdk1 and phosphorylation of p27. Sci Rep 2019; 9: 18693.
[22] Bogenmann E, Moghadam H, DeClerck YA and Mock A. c-myc amplification and expression in newly established human osteosarcoma cell lines. Cancer Res 1987; 47: 3808-3814.
[23] Zhao SJ, Shen YF, Li Q, He YJ, Zhang YK, Hu LP, Jiang YQ, Xu NW, Wang YJ, Li J, Wang YH, Liu F, Zhang R, Yin GY, Tang JH, Zhou D and Zhang ZG. SLIT2/ROBO1 axis contributes to the Warburg effect in osteosarcoma through activation of SRC/ERK/c-MYC/PFKFB2 pathway. Cell Death Dis 2018; 9: 390.
[24] Shimizu T, Ishikawa T, Sugihara E, Kuninaka S, Miyamoto T, Mabuchi Y, Matsuzaki Y, Tsunoda T, Miya F, Morioka H, Nakayama R, Kobayashi E, Toyama Y, Kawai A, Ichikawa H, Hasegawa T, Okada S, Ito T, Ikeda Y, Suda T and Saya H. c-MYC overexpression with loss of Ink4a/Arf transforms bone marrow stromal cells into osteosarcoma accompanied by loss of adipogenesis. Oncogene 2010; 29: 5687-5699.
[25] Jiang Y, Wang J, Sun M, Zuo D, Wang H, Shen J, Jiang W, Mu H, Ma X, Yin F, Lin J, Wang C, Yu S, Jiang L, Lv G, Liu F, Xue L, Tian K, Wang G, Zhou Z, Lv Y, Wang Z, Zhang T, Xu J, Yang L, Zhao K, Sun W, Tang Y, Cai Z, Wang S and Hua Y. Multi-omics analysis identifies osteosarcoma subtypes with distinct prognosis indicating stratified treatment. Nat Commun 2022; 13: 7207.
[26] Shen W, Liang XH, Sun H, De Hoyos CL and Crooke ST. Depletion of NEAT1 lncRNA attenuates nucleolar stress by releasing sequestered P54nrb and PSF to facilitate c-Myc translation. PLoS One 2017; 12: e0173494.
[27] Hu Z, Dong L, Li S, Li Z, Qiao Y, Li Y, Ding J, Chen Z, Wu Y, Wang Z, Huang S, Gao Q, Zhao Y and He X. Splicing regulator p54(nrb)/non-POU domain-containing octamer-binding protein enhances carcinogenesis through oncogenic isoform switch of MYC box-dependent interacting protein 1 in hepatocellular carcinoma. Hepatology 2020; 72: 548-568.
[28] Shen W, Liang XH and Crooke ST. Phosphorothioate oligonucleotides can displace NEAT1

RNA and form nuclear paraspeckle-like structures. Nucleic Acids Res 2014; 42: 8648-8662.
[29] Lauvrak SU, Munthe E, Kresse SH, Stratford EW, Namløs HM, Meza-Zepeda LA and Myklebost O. Functional characterisation of osteosarcoma cell lines and identification of mRNAs and miRNAs associated with aggressive cancer phenotypes. Br J Cancer 2013; 109: 2228-2236.
[30] Davis S and Meltzer PS. GEOquery: a bridge between the Gene Expression Omnibus (GEO) and bioConductor. Bioinformatics 2007; 23: 1846-1847.
[31] Colaprico A, Silva TC, Olsen C, Garofano L, Cava C, Garolini D, Sabedot TS, Malta TM, Pagnotta SM, Castiglioni I, Ceccarelli M, Bontempi G and Noushmehr H. TCGAbiolinks: an R/bioconductor package for integrative analysis of TCGA data. Nucleic Acids Res 2016; 44: e71.
[32] Lei Z, Duan H, Zhao T, Zhang Y, Li G, Meng J, Zhang S and Yan W. PARK2 inhibits osteosarcoma cell growth through the JAK2/STAT3/VEGF signaling pathway. Cell Death Dis 2018; 9: 375.
[33] Cobbold LC, Spriggs KA, Haines SJ, Dobbyn HC, Hayes C, de Moor CH, Lilley KS, Bushell M and Willis AE. Identification of internal ribosome entry segment (IRES)-trans-acting factors for the Myc family of IRESs. Mol Cell Biol 2008; 28: 40-49.
[34] Huang J, Ringuet M, Whitten AE, Caria S, Lim YW, Badhan R, Anggono V and Lee M. Structural basis of the zinc-induced cytoplasmic aggregation of the RNA-binding protein SFPQ. Nucleic Acids Res 2020; 48: 3356-3365.
[35] Fagerberg L, Hallström BM, Oksvold P, Kampf C, Djureinovic D, Odeberg J, Habuka M, Tahmasebpoor S, Danielsson A, Edlund K, Asplund A, Sjöstedt E, Lundberg E, Szigyarto CA, Skogs M, Takanen JO, Berling H, Tegel H, Mulder J, Nilsson P, Schwenk JM, Lindskog C, Danielsson F, Mardinoglu A, Sivertsson A, von Feilitzen K, Forsberg M, Zwahlen M, Olsson I, Navani S, Huss M, Nielsen J, Ponten F and Uhlén M. Analysis of the human tissue-specific expression by genome-wide integration of transcriptomics and antibody-based proteomics. Mol Cell Proteomics 2014; 13: 397-406.
[36] Klotz-Noack K, Klinger B, Rivera M, Bublitz N, Uhlitz F, Riemer P, Lüthen M, Sell T, Kasack K, Gastl B, Ispasanie SSS, Simon T, Janssen N, Schwab M, Zuber J, Horst D, Blüthgen N, Schäfer R, Morkel M and Sers C. SFPQ depletion is synthetically lethal with BRAF(V600E) in colorectal cancer cells. Cell Rep 2020; 32: 108184.
[37] He SW, Xu C, Li YQ, Li YQ, Zhao Y, Zhang PP, Lei Y, Liang YL, Li JY, Li Q, Chen Y, Huang SY, Ma J and Liu N. AR-induced long non-coding RNA LINC01503 facilitates proliferation and metastasis via the SFPQ-FOSL1 axis in nasopharyngeal carcinoma. Oncogene 2020; 39: 5616-5632.
[38] Pellarin I, Dall'Acqua A, Gambelli A, Pellizzari I, D'Andrea S, Sonego M, Lorenzon I, Schiappacassi M, Belletti B and Baldassarre G. Splicing factor proline- and glutamine-rich (SFPQ) protein regulates platinum response in ovarian cancer-modulating SRSF2 activity. Oncogene 2020; 39: 4390-4403.
[39] Biloglav A, Olsson-Arvidsson L, Theander J, Behrendtz M, Castor A and Johansson B. SFPQ-ABL1-positive B-cell precursor acute lymphoblastic leukemias. Genes Chromosomes Cancer 2020; 59: 540-543.
[40] de Silva HC, Lin MZ, Phillips L, Martin JL and Baxter RC. IGFBP-3 interacts with NONO and SFPQ in PARP-dependent DNA damage repair in triple-negative breast cancer. Cell Mol Life Sci 2019; 76: 2015-2030.
[41] Lakiotaki E, Kanakoglou DS, Pampalou A, Karatrasoglou EA, Piperi C and Korkolopoulou P. Dissecting the role of circular RNAs in sarcomas with emphasis on osteosarcomas. Biomedicines 2021; 9: 1642.
[42] Bao Q, Gong L, Wang J, Wen J, Shen Y and Zhang W. Extracellular vesicle RNA sequencing reveals dramatic transcriptomic alterations between metastatic and primary osteosarcoma in a liquid biopsy approach. Ann Surg Oncol 2018; 25: 2642-2651.
[43] Rothzerg E, Ho XD, Xu J, Wood D, Märtson A, Maasalu K and Kõks S. Alternative splicing of leptin receptor overlapping transcript in osteosarcoma. Exp Biol Med (Maywood) 2020; 245: 1437-1443.
[44] Leroy B, Ballinger ML, Baran-Marszak F, Bond GL, Braithwaite A, Concin N, Donehower LA, El-Deiry WS, Fenaux P, Gaidano G, Langerød A, Hellstrom-Lindberg E, Iggo R, Lehmann-Che J, Mai PL, Malkin D, Moll UM, Myers JN, Nichols KE, Pospisilova S, Ashton-Prolla P, Rossi D, Savage SA, Strong LC, Tonin PN, Zeillinger R, Zenz T, Fraumeni JF Jr, Taschner PE, Hainaut P and Soussi T. Recommended guidelines for validation, quality control, and reporting of TP53 variants in clinical practice. Cancer Res 2017; 77: 1250-1260.
[45] Chen K, Li C, Huang S, Chen Y and Zhu X. LncRNA KASRT serves as a potential treatment target by regulating SRSF1-related KLF6 alternative splicing and the P21/CCND1 pathway in osteosarcoma: an in vitro and in vivo study. Front Oncol 2021; 11: 700963.
[46] Ajiro M, Jia R, Yang Y, Zhu J and Zheng ZM. A genome landscape of SRSF3-regulated splicing events and gene expression in human os-

teosarcoma U2OS cells. Nucleic Acids Res 2016; 44: 1854-1870.

[47] Lee JH, Horak CE, Khanna C, Meng Z, Yu LR, Veenstra TD and Steeg PS. Alterations in Gemin5 expression contribute to alternative mRNA splicing patterns and tumor cell motility. Cancer Res 2008; 68: 639-644.

[48] Filippov V, Filippova M and Duerksen-Hughes PJ. The early response to DNA damage can lead to activation of alternative splicing activity resulting in CD44 splice pattern changes. Cancer Res 2007; 67: 7621-7630.

[49] Torres S, García-Palmero I, Marín-Vicente C, Bartolomé RA, Calviño E, Fernández-Aceñero MJ and Casal JI. Proteomic characterization of transcription and splicing factors associated with a metastatic phenotype in colorectal cancer. J Proteome Res 2018; 17: 252-264.

[50] Xu Y, Karlsson A and Johansson M. Identification of genes associated to 2',2'-difluorodeoxycytidine resistance in HeLa cells with a lentiviral short-hairpin RNA library. Biochem Pharmacol 2011; 82: 210-215.

[51] Francica P, Mutlu M, Blomen VA, Oliveira C, Nowicka Z, Trenner A, Gerhards NM, Bouwman P, Stickel E, Hekkelman ML, Lingg L, Klebic I, van de Ven M, de Korte-Grimmerink R, Howald D, Jonkers J, Sartori AA, Fendler W, Chapman JR, Brummelkamp T and Rottenberg S. Functional radiogenetic profiling implicates ERCC6L2 in non-homologous end joining. Cell Rep 2020; 32: 108068.

[52] Miller DM, Thomas SD, Islam A, Muench D and Sedoris K. c-Myc and cancer metabolism. Clin Cancer Res 2012; 18: 5546-5553.

[53] Han G, Wang Y and Bi W. C-Myc overexpression promotes osteosarcoma cell invasion via activation of MEK-ERK pathway. Oncol Res 2012; 20: 149-156.

[54] Scionti I, Michelacci F, Pasello M, Hattinger CM, Alberghini M, Manara MC, Bacci G, Ferrari S, Scotlandi K, Picci P and Serra M. Clinical impact of the methotrexate resistance-associated genes C-MYC and dihydrofolate reductase (DHFR) in high-grade osteosarcoma. Ann Oncol 2008; 19: 1500-1508.

[55] Nelson LD, Bender C, Mannsperger H, Buergy D, Kambakamba P, Mudduluru G, Korf U, Hughes D, Van Dyke MW and Allgayer H. Triplex DNA-binding proteins are associated with clinical outcomes revealed by proteomic measurements in patients with colorectal cancer. Mol Cancer 2012; 11: 38.

[56] Zhang Y, Wu D and Wang D. Long non-coding RNA ARAP1-AS1 promotes tumorigenesis and metastasis through facilitating proto-oncogene c-Myc translation via dissociating PSF/PTB dimer in cervical cancer. Cancer Med 2020; 9: 1855-1866.